

ChemComm

Chemical Communications

Accepted Manuscript

This article can be cited before page numbers have been issued, to do this please use: N. E. Leydman and P. L. Norcott, *Chem. Commun.*, 2024, DOI: 10.1039/D4CC03231D.



This is an Accepted Manuscript, which has been through the Royal Society of Chemistry peer review process and has been accepted for publication.

Accepted Manuscripts are published online shortly after acceptance, before technical editing, formatting and proof reading. Using this free service, authors can make their results available to the community, in citable form, before we publish the edited article. We will replace this Accepted Manuscript with the edited and formatted Advance Article as soon as it is available.

You can find more information about Accepted Manuscripts in the [Information for Authors](#).

Please note that technical editing may introduce minor changes to the text and/or graphics, which may alter content. The journal's standard [Terms & Conditions](#) and the [Ethical guidelines](#) still apply. In no event shall the Royal Society of Chemistry be held responsible for any errors or omissions in this Accepted Manuscript or any consequences arising from the use of any information it contains.

COMMUNICATION

Aldoximes Enable Proton-Relayed NMR Hyperpolarisation

Naomi E. Leydman^a and Philip L. Norcott*^aReceived 00th January 20xx,
Accepted 00th January 20xx

DOI: 10.1039/x0xx00000x

NMR signals can be greatly enhanced, or hyperpolarised, by interactions with para-hydrogen. We demonstrate here that oximes can be reversibly hyperpolarised by coordination to an iridium complex, that oxime *E/Z* geometry is significant for activity, and that hyperpolarised oximes can subsequently transfer these enhanced signals through proton exchange.

A significant increase to the signal strength in nuclear magnetic resonance (NMR) spectroscopy and magnetic resonance imaging (MRI) can be achieved through hyperpolarisation.¹ Typically, in an external magnetic field the bulk polarisation of a sample is very small, resulting in low sensitivity. This occurs from the small population difference between Zeeman-split states under thermal (Boltzmann) conditions. Perturbation of this thermal distribution by some means can lead to far larger population differences and accordingly a greater bulk magnetisation, that is, hyperpolarisation. This produces signals that may be orders of magnitude greater in intensity, a valuable feature currently being explored for clinical imaging and metabolic monitoring,^{2, 3} or for the enhanced detection of biologically-relevant analytes,^{4, 5} or for measurements at low magnetic field strengths.^{6, 7}

Several methods of hyperpolarisation exist, but a particularly accessible and affordable method involves para-hydrogen (*p*-H₂), an isomer of hydrogen gas with a non-thermal nuclear spin order.⁸ Addition reactions with *p*-H₂ can result in a hyperpolarised hydrogenation product,⁹ a process known as Para-Hydrogen Induced Polarisation (PHIP) which has been studied in the context of both homogeneous and heterogeneous catalysis.^{10, 11} An important non-hydrogenative variant of PHIP is Signal Amplification By Reversible Exchange (SABRE), where *p*-H₂ and a target molecule can reversibly associate with a metal

complex, allowing transfer of hyperpolarised magnetisation through the temporary *J*-coupling of the complex without chemically modifying the target.^{12, 13} Normally, a requirement for this process is the target must have a suitable coordinating affinity to the metal centre, but it has also been shown that certain molecules capable of donating or accepting protons can deliver and/or accept SABRE hyperpolarisation via this exchange (a 'relay' step).^{14, 15}

Here, we demonstrate that aldoximes are amenable ligands for SABRE (Figure 1), revealing the key properties that influence hyperpolarisation level, the active catalyst species, and the ability and utility of oximes to engage in SABRE-Relay.

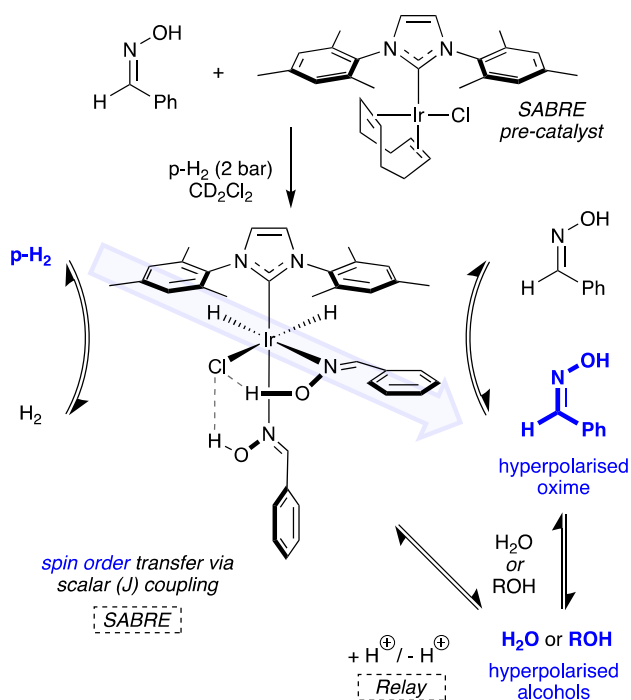


Figure 1: Transfer of hyperpolarised magnetisation from *p*-H₂ to oximes via an iridium complex, followed by signal transfer via proton exchange.

^a Research School of Chemistry, Australian National University, 2601 Canberra, ACT, Australia. E-mail: philip.norcott@anu.edu.au

† Electronic Supplementary Information (ESI) available: See DOI: 10.1039/x0xx00000x.



Oximes are oxygenated imine analogues widely used in organic synthesis,¹⁶ coordination chemistry,¹⁷ and notably as antidotes against organophosphate poisoning.¹⁸ To begin our study, we sought to react the benzaldehyde oxime **1** (Figure 2) with the commonly used SABRE pre-catalyst [IrCl(COD)(IMes)] (COD = 1,5-*cis,cis*-cyclooctadiene, IMes = 1,3-bis(2,4,6-trimethylphenyl)imidazol-2-ylidene). In conventional SABRE under H₂ an Ir(III) dihydride species is formed and following COD hydrogenation three sites are available for coordination of a target molecule. For **1**, we anticipated that the oxime geometry would dramatically affect the coordinating ability as *E* and *Z* forms would exhibit very different steric environments.

The reaction of benzaldehyde dimethyl acetal with hydroxylamine hydrochloride gave two isomers of oxime **1** which could be readily separated chromatographically, but in our hands dissolution of either product in CDCl₃ revealed equilibrium mixtures of *E* and *Z* oximes. Dissolution in *d*₆-DMSO or CD₂Cl₂, however, prevented any equilibration in solution.

With *E*-**1** and *Z*-**1** in hand, we combined each oxime (30 mM) with [IrCl(COD)(IMes)] (10 mM) in CD₂Cl₂. The sample was shaken under p-H₂ (2 bar) for 10 seconds at 65 G then immediately transferred to a 1.4 T (60 MHz) NMR spectrometer and acquisition of a single-scan ¹H spectrum. As seen in Figure 2a, *Z*-**1** was significantly more effective than *E*-**1**, showing hyperpolarised oxime responses with signal enhancements of 113-fold over the normal spectrum for *Z*-**1**, compared to only 6-fold for *E*-**1**. The weaker hyperpolarisation for *E*-**1** supports our steric argument, and is reminiscent of recent reports of the dependence on *E* and *Z* azobenzenes for SABRE activity, with a preference for the less sterically encumbered *Z* isomer.¹⁹

Interestingly, a hyperpolarised peak corresponding to H₂O (1.5 ppm), presumably present in trace amounts in the solvent, could also be observed. We recognised that a response at this chemical shift may also correspond to hyperpolarised cyclooctane (a PHIP result rather than SABRE), but to refute this we found that repeated treatments with fresh p-H₂ continued to give this hyperpolarised resonance even after the sample was left to react completely for several days under H₂ while high-field NMR analysis revealed complete consumption of COD within minutes to an hour. A hyperpolarised o-H₂ resonance (4.6 ppm) is also observed, indicating reversible addition and elimination of dihydrogen.

At a higher detection field (400 MHz), additional hyperpolarised responses corresponding to bound oxime ligands were also detected (Figure 2b). These are consistent with a catalyst structure of the form [IrCl(H)₂(IMes)(*Z*-**1**)₂] which is supported by Density Functional Theory (DFT) calculations (Figure 2c, *vide infra*). A bound oxime ligand *cis* to the IMes ligand (*Z*-**1**_{eq}) was enhanced by a similar amount to the free oxime ligand (around 50-fold at the N=CH position), while those of the oxime *trans* to the IMes (*Z*-**1**_{ax}) showed weaker but measurable hyperpolarisation (only 10-fold enhancement). This may be in part due to a slower ligand exchange at this position, which we have also observed through exchange spectroscopy (EXSY) measurements, and is supported by a brief examination of polarisation transfer at an increased temperature which increases enhancement (Supporting Information, section 1.4).

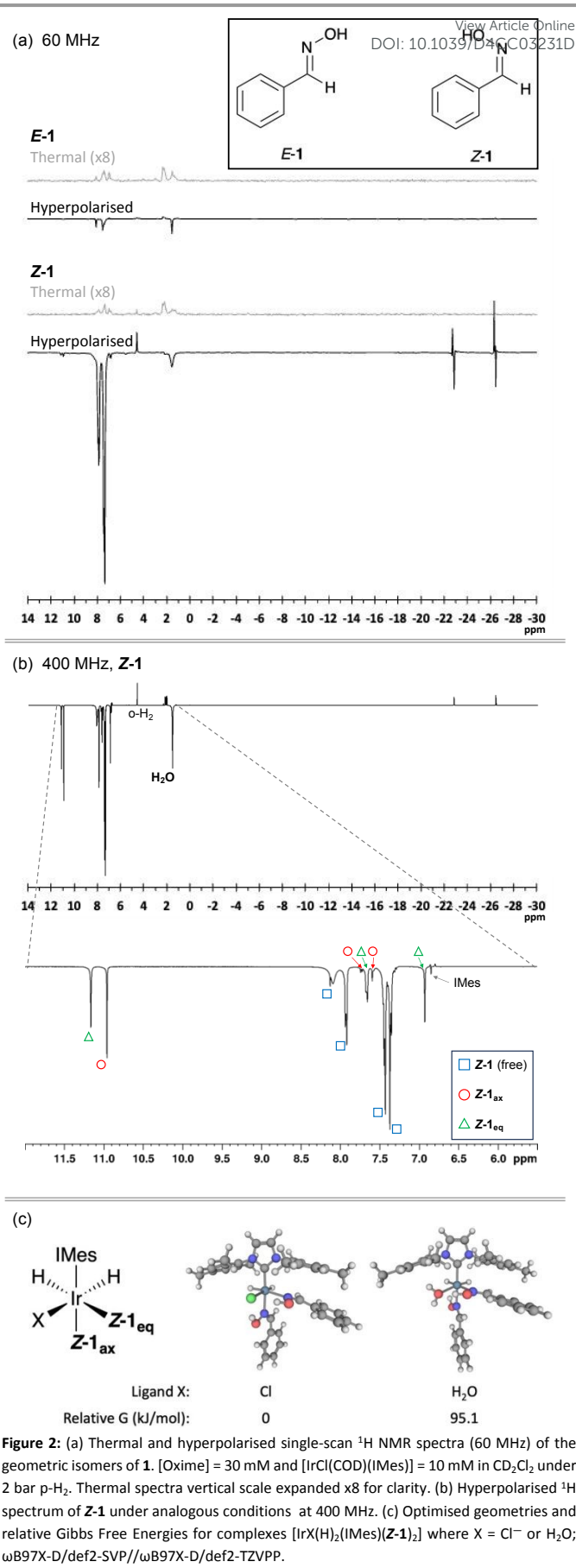


Figure 2: (a) Thermal and hyperpolarised single-scan ¹H NMR spectra (60 MHz) of the geometric isomers of **1**. [Oxime] = 30 mM and [IrCl(COD)(IMes)] = 10 mM in CD₂Cl₂ under 2 bar p-H₂. Thermal spectra vertical scale expanded x8 for clarity. (b) Hyperpolarised ¹H spectrum of *Z*-**1** under analogous conditions at 400 MHz. (c) Optimised geometries and relative Gibbs Free Energies for complexes [IrX(H)₂(IMes)(*Z*-**1**)₂] where X = Cl⁻ or H₂O; ωB97X-D/def2-SVP//ωB97X-D/def2-TZVPP.



The notable exception to this trend was the OH responses of both bound ligands, which were more consistently hyperpolarised (each approximately 70-fold enhancement), which is a similar magnitude to the free oxime OH and H₂O itself. The imidazole of the NHC only exhibited very weak hyperpolarisation. Details of enhancement values, assignments of this complex, and a screen of the polarisation transfer field can be found in Appendix S2 of the Supporting Information.

In addition to the steric differences between *E/Z* isomers, oximes of different electronic properties were also investigated: a (*p*-OMe)-phenyl (**2**) and a (*p*-CF₃)-phenyl (**3**) analogue to probe more electron-rich and electron-deficient oximes, respectively (Appendix S3 in the Supporting Information). In both cases, the *Z* isomers were superior to the corresponding *E* isomers. The most notable electronic effect was the withdrawing CF₃ functional group on **3** reduced the SABRE activity significantly, with **Z-3** showing hyperpolarised hydrides but little else. However, the presence of a donating OMe functional group on **2** did not reveal a dramatic change compared to the unfunctionalised compound **1**, with **Z-2** displaying oxime resonances enhanced by only 28-fold. For analogues bearing multiple OMe groups, the increased size appeared to hinder any advantage that may have been gained from electronic effects.

To support the identity of the reactive species during these processes, we investigated the most effective of these analogues, **Z-1**, more closely. Thermally polarised spectra at 400 MHz reveal that only 2 equivalents of oxime coordinate to iridium (see Appendix S1). This is consistent with the observed inequivalent hydride resonances at -22.7 and -26.4 ppm, suggesting a non-symmetrical complex of the form [IrX(H)₂(IMes)(**Z-1**_{ax})(**Z-1**_{eq})], where ax = axial, eq = equatorial (Figure 2c), and X is a ligand we considered plausibly could be Cl⁻, H₂O, or a chelation mode. 2D EXSY revealed only the equatorially bound **Z-1**_{eq} exchanges with free **Z-1**. Two sharp resonances indicating intramolecularly hydrogen-bonded OH groups each from **Z-1**_{ax} and **Z-1**_{eq} (11.0 and 11.2 ppm) also showed an exchange interaction with free H₂O.

To differentiate between an active complex with a bound H₂O or Cl in the X site, CD₂Cl₂ that had been dried over CaH₂ followed by 4Å MS was used to exclude all spurious water from the solvent. Even when this SABRE sample was doped with 2 eq. MeOH (with respect to Ir) an identical complex was revealed, with no discernible difference in the chemical shift of the hydrides, suggesting a bound H₂O is less plausible. The reaction with p-H₂, notably, now produced a strong hyperpolarised MeOH response with the methyl group enhanced by 173-fold over the thermal spectrum (see Appendix S3).

DFT calculations also suggest the more thermodynamically stable complex is [IrCl(H)₂(IMes)(**Z-1**)₂], rather than [Ir(H₂O)(H)₂(IMes)(**Z-1**)₂Cl], by 95.1 kJ.mol⁻¹ (Figure 2c). We were unable to find any reasonable structures with bidentate oxime *N,O*-coordination. The lowest energy conformer of the preferred complex displayed two intramolecular hydrogen-bonding interactions with the adjacent Cl, consistent with our previously discussed spectroscopic observations. Structures were optimised with a continuum solvation model (SMD)²⁰ in dichloromethane using the ωB97X-D functional²¹ and def2-SVP

basis set.²² Subsequent single point energies were calculated using the def2-TZVPP basis set. DOI: 10.1039/D4CC03231D

These studies therefore suggest that the observed hyperpolarisation of H₂O or MeOH is through a SABRE-Relay process (via proton exchange), rather than directly through an Ir-bound H₂O or MeOH. We also found that *n*-butanol participated in a similar fashion. There have already been fairly comprehensive studies of different substrates containing exchangeable protons that participate in SABRE-Relay where primary amines are used to coordinate to iridium,¹⁴ and from our results we would expect a similar scope to be possible here.

However, the consistent OH hyperpolarisation levels between bound and free oxime ligands and H₂O identified earlier in this work suggest the SABRE relay mechanism may also exhibit some distinguishing features. In particular, it is possible proton exchange to water or alcohols may proceed directly from the Ir catalyst, without oxime dissociation being strictly necessary. In particular, the exchange spectroscopy measurements available in Appendix 1 of the Supporting Information reveal proton exchange between the axially-bound OH resonance and H₂O, despite slow dissociation of this ligand from the metal centre. The ability to deliver proton-relayed hyperpolarisation in part disconnected from the rate of organic ligand dissociation may be a promising alternative strategy to conventional SABRE-Relay in future work.

It is evident that the role of oximes in these examples is as the 'mediator' in the SABRE-Relay process: a molecule able to coordinate Ir to acquire SABRE-derived magnetisation then to discharge it via proton-transfer to a 'target' (alcohols in this case), according to the terminology we show in the general sequence in Figure 3a. However, we also wanted to see if oximes could act as 'targets' (poorly binding to Ir, but receiving hyperpolarised magnetisation via proton transfer). This would allow signal enhancement of even the more sterically hindered *E*-isomers we investigated at the outset of this work.

As such, we prepared a sample of **1** (30 mM) consisting of an equilibrium mixture of *E:Z* isomers present in a 14:1 ratio and [IrCl(COD)(IMes)] (10 mM) in CD₂Cl₂ for SABRE as before. Whereas pure *E-1* originally performed poorly, the 14:1 *E:Z* mixture gave much improved hyperpolarised signal responses (Figure 3c). We propose that steric constraints force only the *Z* isomer to act as SABRE-Relay *mediator* while proton exchange allows the *E* isomer to act as the *target*. Indeed, from this mixture we could not detect any hyperpolarised free **Z-1** as this is presumably iridium-bound (noting the identical resonances in the hydride region in Figure 3c), and we observed only hyperpolarised free *E-1*. We suggest that this is a crucial consideration given our observations of the propensity of oximes to isomerise even under weakly acidic conditions, as future applications in this area may likely involve (intentionally or unintentionally) thermodynamic mixtures of *E* and *Z* compounds. Further DFT modelling revealed that for competitive binding in a mixture of *E* and *Z* oximes, coordination by **Z-1** was thermodynamically preferred, but that complexes with mixed ligand speciation such as [IrCl(H)₂(IMes)(**Z-1**)(*E-1*)] (refer to Appendix 4) cannot be discounted as also contributing to this effect.



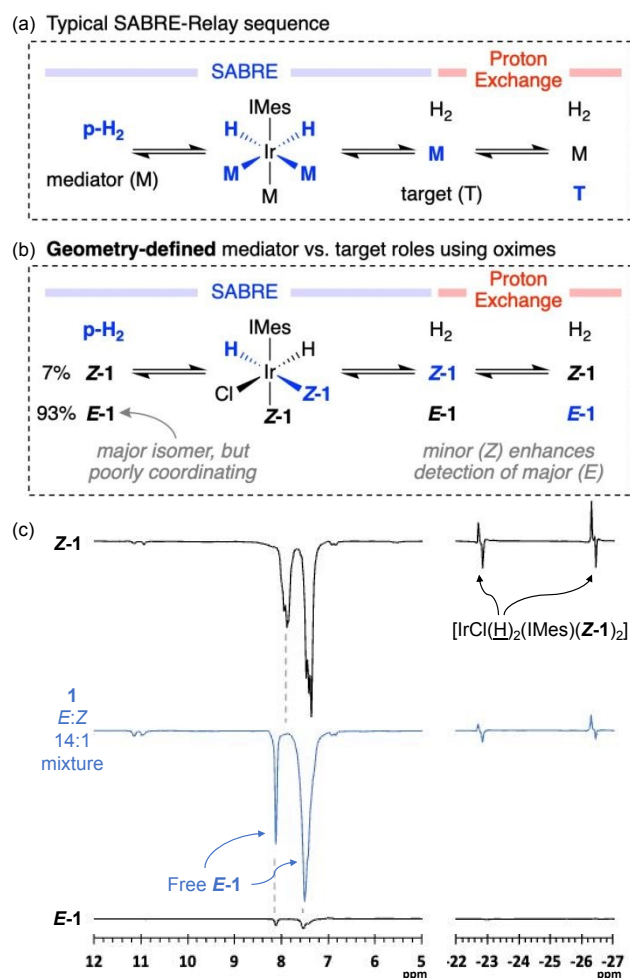


Figure 3: (a) Typical roles of mediator and target in SABRE-Relay, with (b) geometric isomers of oximes playing different roles. (c) Hyperpolarised ^1H NMR spectra of a mixture of E and Z isomers of oxime 1.

In conclusion, we have shown that aldoximes are amenable to SABRE using the most common iridium catalyst, with the Z-configured oxime playing the primary role of coordination. The pendant OH on these molecules provides a route for transfer of hyperpolarised magnetisation both to and from oximes via proton exchange. Investigations into related derivatives are ongoing in our laboratory, and will be reported in due course.

P. L. N. gratefully acknowledges a Discovery Early Career Researcher Award (DECRA) from the Australian Research Council (DE210100065). This work was undertaken with the assistance of resources and services from the National Computational Infrastructure (NCI), which is supported by the Australian Government. N. E. L. conducted synthetic and analytical experiments and reviewed the manuscript. P. L. N. conceived the project, wrote the initial draft, and performed synthetic, analytical and computational experiments.

Data Availability

Raw NMR data files supporting this work are openly available in the Australian National University Data Commons located at <https://datacommons.anu.edu.au> (10.25911/5c3t-7137).

Conflicts of interest

There are no conflicts to declare.

Notes and references

- J. Eills, D. Budker, S. Cavagnero, E. Y. Chekmenev, S. J. Elliott, S. Jannin, A. Lesage, J. Matysik, T. Meersmann, T. Prisner, J. A. Reimer, H. Yang and I. V. Koptug, *Chem. Rev.*, 2023, **123**, 1417-1551.
- H. de Maissin, P. R. Groß, O. Mohiuddin, M. Weigt, L. Nagel, M. Herzog, Z. Wang, R. Willing, W. Reichardt, M. Pichotka, L. Heß, T. Reinheckel, H. J. Jessen, R. Zeiser, M. Bock, D. von Elverfeldt, M. Zaitsev, S. Korchak, S. Glögger, J.-B. Hövener, E. Y. Chekmenev, F. Schilling, S. Knecht and A. B. Schmidt, *Angew. Chem., Int. Ed.*, 2023, **62**, e202306654.
- K. MacCulloch, A. Browning, D. O. Guarín Bedoya, S. J. McBride, M. B. Abdulmojeed, C. Dedesma, B. M. Goodson, M. S. Rosen, E. Y. Chekmenev, Y.-F. Yen, P. TomHon and T. Theis, *J. Magn. Reson. Open*, 2023, **16-17**, 100129.
- N. Reimets, K. Ausmees, S. Vija, A. Trummal, M. Uudsemaa and I. Reile, *Analyst*, 2023, **148**, 5407-5415.
- A. Alshehri, B. J. Tickner, W. Iali and S. B. Duckett, *Chem. Sci.*, 2023, **14**, 9843-9853.
- R. Kircher, J. Xu and D. A. Barskiy, *J. Am. Chem. Soc.*, 2024, **146**, 514-520.
- N. Iqbal, D. O. Brittin, P. J. Daluwathumullagamage, M. S. Alam, I. M. Senanayake, A. T. Gafar, Z. Siraj, A. Petrilla, M. Pugh, B. Tonazzi, S. Ragunathan, M. E. Poorman, L. Sacolick, T. Theis, M. S. Rosen, E. Y. Chekmenev and B. M. Goodson, *Anal. Chem.*, 2024, DOI: 10.1021/acs.analchem.4c01299.
- G. Buntkowsky, F. Theiss, J. Lins, Y. A. Miloslavina, L. Wienands, A. Kiryutin and A. Yurkovskaya, *RSC Adv.*, 2022, **12**, 12477-12506.
- C. R. Bowers and D. P. Weitekamp, *J. Am. Chem. Soc.*, 1987, **109**, 5541-5542.
- E. V. Pokochueva, D. B. Burueva, O. G. Salnikov and I. V. Koptug, *ChemPhysChem*, 2021, **22**, 1421-1440.
- B. J. Tickner and V. V. Zhivonitko, *Chem. Sci.*, 2022, **13**, 4670-4696.
- R. W. Adams, J. A. Aguilar, K. D. Atkinson, M. J. Cowley, P. I. P. Elliott, S. B. Duckett, G. G. R. Green, I. G. Khazal, J. López-Serrano and D. C. Williamson, *Science*, 2009, **323**, 1708-1711.
- P. J. Rayner and S. B. Duckett, *Angew. Chem., Int. Ed.*, 2018, **57**, 6742-6753.
- W. Iali, P. J. Rayner and S. B. Duckett, *Sci. Adv.*, 2018, **4**, eaao6250.
- P. J. Rayner, B. J. Tickner, W. Iali, M. Fekete, A. D. Robinson and S. B. Duckett, *Chem. Sci.*, 2019, **10**, 7709-7717.
- D. K. Kölmel and E. T. Kool, *Chem. Rev.*, 2017, **117**, 10358-10376.
- V. Y. Kukushkin and A. J. L. Pombeiro, *Coord. Chem. Rev.*, 1999, **181**, 147-175.
- G. Mercey, T. Verdet, J. Renou, M. Kliachyna, R. Baati, F. Nachon, L. Jean and P.-Y. Renard, *Acc. Chem. Res.*, 2012, **45**, 756.
- A. S. Kiryutin, V. P. Kozinenko and A. V. Yurkovskaya, *ChemPhotoChem*, 2024, **8**, e202300151.
- A. V. Marenich, C. J. Cramer and D. G. Truhlar, *J. Phys. Chem. B*, 2009, **113**, 6378-6396.
- J.-D. Chai and M. Head-Gordon, *Phys. Chem. Chem. Phys.*, 2008, **10**, 6615-6620.
- F. Weigend and R. Ahlrichs, *Phys. Chem. Chem. Phys.*, 2005, **7**, 3297-3305.



Raw NMR data files supporting this work are openly available in the Australian National University Data Commons located at <https://datacommons.anu.edu.au> (10.25911/5c3t-7137).

View Article Online

DOI: 10.1039/D4CC03231D

